IOP Conf. Series: Materials Science and Engineering **181** (2017) 012022 doi:10.1088/1757-899X/181/1/012022

A numerical and experimental study of temperature effects on deformation behavior of carbon steels at high strain rates

M Pouya, S Winter, S Fritsch and M F-X Wagner

Chemnitz University of Technology, Institute of Materials Science and Engineering, 09125 Chemnitz, Germany

Abstract. Both in research and in the light of industrial applications, there is a growing interest in methods to characterize the mechanical behavior of materials at high strain rates. This is particularly true for steels (the most important structural materials), where often the strain rate-dependent material behavior also needs to be characterized in a wide temperature range. In this study, we use the Finite Element Method (FEM), first, to model the compressive deformation behavior of carbon steels under quasi-static loading conditions. The results are then compared to experimental data (for a simple C75 steel) at room temperature, and up to testing temperatures of 1000 °C. Second, an explicit FEM model that captures wave propagation phenomena during dynamic loading is developed to closely reflect the complex loading conditions in a Split-Hopkinson Pressure Bar (SHPB) – an experimental setup that allows loading of compression samples with strain rates up to 10^4 s^{-1}The dynamic simulations provide a useful basis for an accurate analysis of dynamically measured experimental data, which considers reflected elastic waves. By combining numerical and experimental investigations, we derive material parameters that capture the strain rate- and temperature-dependent behavior of the C75 steel from room temperature to 1000 °C, and from quasi-static to dynamic loading.

1. Introduction

It is well known that during dynamic loading the mechanical behavior of many materials (like carbon steels, the most important structural materials) differs substantially from that under quasi-static conditions. Due to various industrial applications, e.g. in crash-absorbing structural members, the interest to accurately determine the material behavior at high strain rates has strongly increased during recent decades. Combined with high temperatures, a better understanding of the mechanical behavior is also required to determine the material properties during various manufacturing and production processes. For dynamic testing, different experimental techniques for uniaxial compression are well established. In contrast to the conventional uniaxial testing machines used for quasi-static testing, these techniques (including the drop weight testers and the well-known Split-Hopkinson Pressure Bar setup) enable the material properties to be determined at high strain rates. The Split-Hopkinson Pressure Bar (SHPB) is an ideal tool to apply a controlled impulse of energy on a specimen and thus to determine the dynamic mechanical behavior at strain rates of up to 10^4 s^{-1}. This experimental technique has been used widely, typically at room temperature (RT) [1]. Fewer results have been reported on SHPB testing at higher temperatures [2]. The experimental results at high temperatures appear to be more complicated to analyze because of various experimental effects that occur during the sample heating process and subsequent dynamic loading. Numerical simulations, and a careful comparison between the experimental and numerical results [3, 4], are essential to separate different

effects caused by e.g. measurement techniques, testing machine setup, sample geometry and the material behavior both on the macro- and micro-scale [5, 6].
In this study, a simulation using the Finite Element Method (FEM) is performed to model the compressive deformation behavior of the high strength carbon spring steel C75 under quasi-static loading. The numerical results are compared to those of experiments at RT and at higher temperatures. To capture the complex dynamic loading conditions, an explicit FEM model of the SHPB is developed. The simulations are thereafter expanded to study the effect of higher temperatures under dynamic loading. The dynamic simulations provide an improved theoretical basis for an accurate analysis of dynamically measured experimental data.

2. Experimental and theoretical methods

To study the mechanical behavior of the high strength carbon spring steel C75, cylindrical specimens with a height of 6 mm and a diameter of 4 mm (provided by Risse + Wilke Kaltband GmbH & Co.KG, Iserlohn, Germany) in a hardened and tempered condition were used. The chemical composition was determined by spectroscopic analysis as 0.72 wt.-% C, 0.29 wt.-% Si and 0.74 wt.-% Mn. The material samples were first uniaxially deformed under quasi-static (initial strain rate: 10^{-3} s^{-1}) and dynamic compressive loading conditions. The measured displacements and loads were related to initial sample height and cross section in order to determine engineering strains ε_{eng} and stresses σ_{eng}, respectively (see [7] for further experimental details). Then, true (logarithmic) strains and stresses were calculated from the engineering data. Quasi-static and dynamic compression tests were performed at RT and also at higher temperatures up to 1000 °C. The dynamic compressive tests were conducted using a SHPB with strain rates up to 10^{4} s^{-1}.

The well-known SHPB setup is shown in figure 1. The SHPB system contains a gas launcher, the striker, incident and transmitter bars, and a shock absorber, all of them mounted on a flat base (figure 1a). The test specimen is positioned between the incident and transmitter bars. The gas launcher is charged with a pressurized gas to accelerate the striker bar at a measured velocity and therefore to create an elastic stress pulse. The generated elastic wave pulse (a longitudinal wave) propagates through the incident bar at the speed of sound as determined by the bar material; part of this pulse is reflected at the end of the bar due to impedance mismatches while the other part propagates through the material sample and into the transmitter bar. To prevent signal oscillations, a "pulse shaper" (shown in figure 1b) is embedded between the striker and incident bars. To perform high temperature mechanical testing, the specimen is protected using two ceramic pieces and heated quickly up to a specific testing temperature. Strain gauges (SGs) are positioned on the surfaces of the incident and transmitter bars to measure the strains and the amplitudes of the elastic wave pulse (input and reflected signals in addition to the transmitted signal). Stress and strain values can then be calculated from the data collected by these SGs.

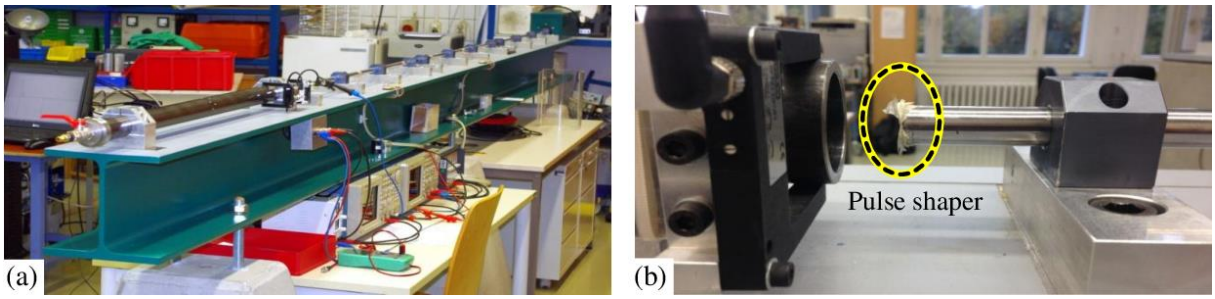

Figure 1. Experimental setup of the SHPB for dynamic compressive loading at high strain rates up to 10^{4} s^{-1} (a). A pulse shaper is embedded between the striker and incident bars to prevent signal oscillations during experimental mechanical testing (b).

The experimental results from quasi-static loading were used as hardening curves in a simple isotropic elastic-plastic material model to simulate the quasi-static thermo-mechanical behavior of C75 using the Abaqus software package. Standard linearly coupled temperature-displacement elements (C3D8T) were employed. Separate simulations were performed, allowing a predefined temperature field (e.g. RT, 200 °C, 400 °C, 600 °C and 800 °C) to reflect the coupled thermo-mechanical behavior of C75 during compressive loading. To capture the dynamic compressive deformation behavior of C75 numerically, the exact experimental setup of the SHPB was carefully defined in Abaqus dynamic explicit, as shown schematically in figure 2.

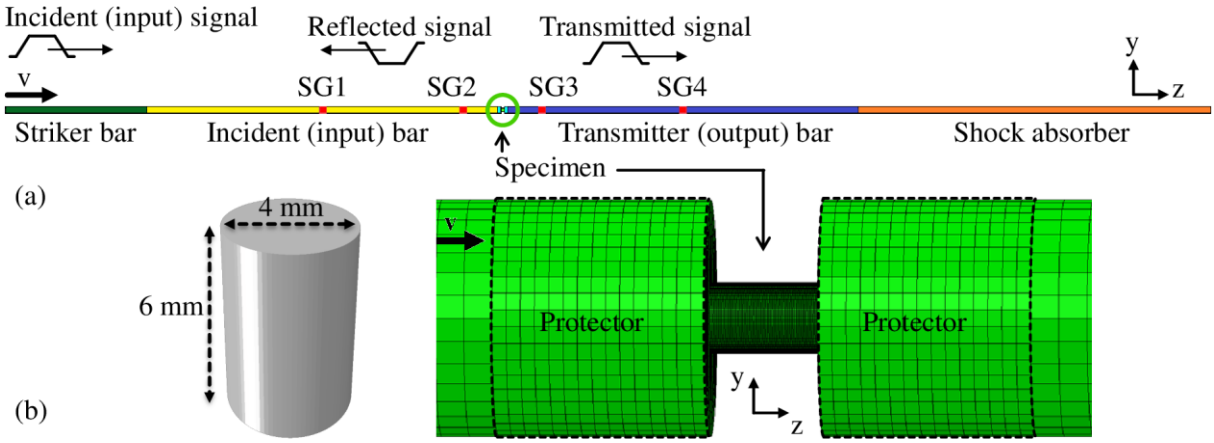

Figure 2. (a) Schematic representation of the simulated SHPB setup. (b) Geometry, mesh and boundary conditions of C75 specimen for the simulation of dynamic compressive loading in the SHPB setup.

The simulated SHPB setup (figure 2a) is a combination of four bars with the same diameter D = 16 mm. All bars consist of the same material, since no wave reflections alone through the SHPB setup is desired. The total length of shock absorber beside the incident and transmitter bars is 1250 mm, while the striker bar has a total length of 500 mm. That ratio of lengths is chosen because the input signal, which contains a double total length of the striker bar, must be able to fit in and travel through the incident bar entirely [8]. The end/front faces of the incident/transmitter bars are protected using two protectors (figure 2b, right; marked by dashed lines), which are replaced by two ceramic pieces at higher temperatures (up to 1000 °C) according to the experimental setup. The effect of the pulse shaper is ignored in our finite element simulations for the sake of simplicity. The striker bar is accelerated dynamically (boundary conditions are defined in terms of velocity) to strike the incident bar. The compression specimen is positioned between the incident and transmitter bar (figure 2b). Based on the real-life experimental setup, the strain gauges number 1 and 4 (SG1 & 4) are positioned in the middle of the incident and transmitter bars (625 mm from end/front faces of incident/transmitter bars) and SG2 and 3 are located closer to the specimen (150 mm from the end/front faces).

Various coupled thermo-mechanical simulations at different test temperatures (RT, 200 °C, 400 °C, 600 °C, 800 °C and 1000 °C) were carried out. Note that the effect of high strain rates was incorporated in the simulations by iteratively adapting the strain rate sensitivity for the RT data (see also figure 3) for a good fit of experimental and simulation results; a constant strain rate sensitivity of m = 0.0062 was assumed for all temperatures and included in the simulations by changing the hardening curves for high strain rate deformation accordingly.

3. Results and Discussion

The experimental and numerically fitted results (true stress as a function of true plastic strain) for quasi-static loading are presented in figure 3. The true stress-strain curves are shown at different temperatures of RT, 200 °C, 400 °C, 600 °C and 800 °C. The flow stresses decrease at higher temperatures during quasi-static loading. The resulting numerical quasi-static material model was used to describe the mechanical behavior of the C75 specimen (positioned in SHPB setup) in the dynamic simulations.

To validate the simulated setup of the SHPB, a "test shot" without a specimen was performed experimentally. The resulting elastic wave pulses are compared to those of a corresponding simulation in figure 4a. Because no specimen is placed in the SHPB system, no reflection of the elastic wave pulse is observed. Therefore the experimental data obtained using a pulse shaper (figure 4a, upper part) and the numerical results (figure 4a, below, ignoring the effect of a pulse shaper) represent only the input and output signals during the test shot. Because of the different positions of the SGs, the elastic pulse data occur at different times in each individual SG.

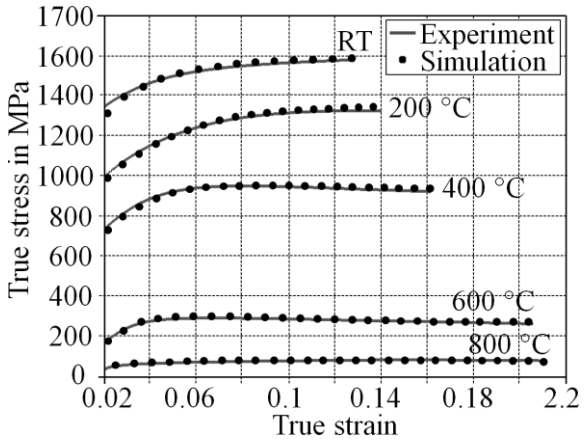

Figure 3. Experimental and numerical true stress-strain curves of quasi-static compression tests at different temperatures (RT, 200 °C, 400 °C, 600 °C and 800 °C). The simulation has been fitted to the experimental (engineering) stress-strain curves.

The propagation of the elastic wave pulse, measured during a regular test and therefore including the compressive dynamic response of the C75 specimen at RT, is presented in figure 4b. The resulting input, reflected and output experimental signals (figure 4b, left) are compared to those of the simulation (figure 4b, right) at the four SGs. With excellent agreement between experiment and simulation, it can be seen that compared to the test shot, by positioning the C75 compression specimen in the SHPB setup, a part of the elastic wave pulse is reflected at the specimen front face. The resulting signal at SG1 consists of both the input and the reflected pulses, while the signal measured in SG2 is a combination of these signals and shifted in time according to its location in the SHPB setup. Therefore the reflected signal at SG1 can be used to calculate the true strains in the specimen. Using the signals measured in SGs 3 and 4, the transmitted mechanical behavior of the specimen is recorded and finally used to calculate true stresses.

The dynamic compressive response of the C75 specimen at RT and higher temperatures (200 °C, 400 °C, 600 °C, 800 °C and 1000 °C) is presented in figure 5, where true stress is plotted as a function of true strain. Since a clear determination of the transition from elastic to plastic behavior is difficult because of the signal oscillations, strains above 0.2 percent are considered to represent plastic deformation. In both experimental and numerical investigations, the true stress-strain curves exhibit strain hardening up to a maximum true stress and afterwards decrease to a steady state response (i.e., negligible hardening). The stress peak marked in the experimental curves (highlighted with an arrow for the curve measured at 800 °C) is not observed in the simulation results. Possible explanations for this experimental effect are geometrical imperfections and/ or misalignment of the compression specimens. Further experimental and theoretical work may be required to fully clarify this effect, which is frequently observed experimentally at increased temperatures.

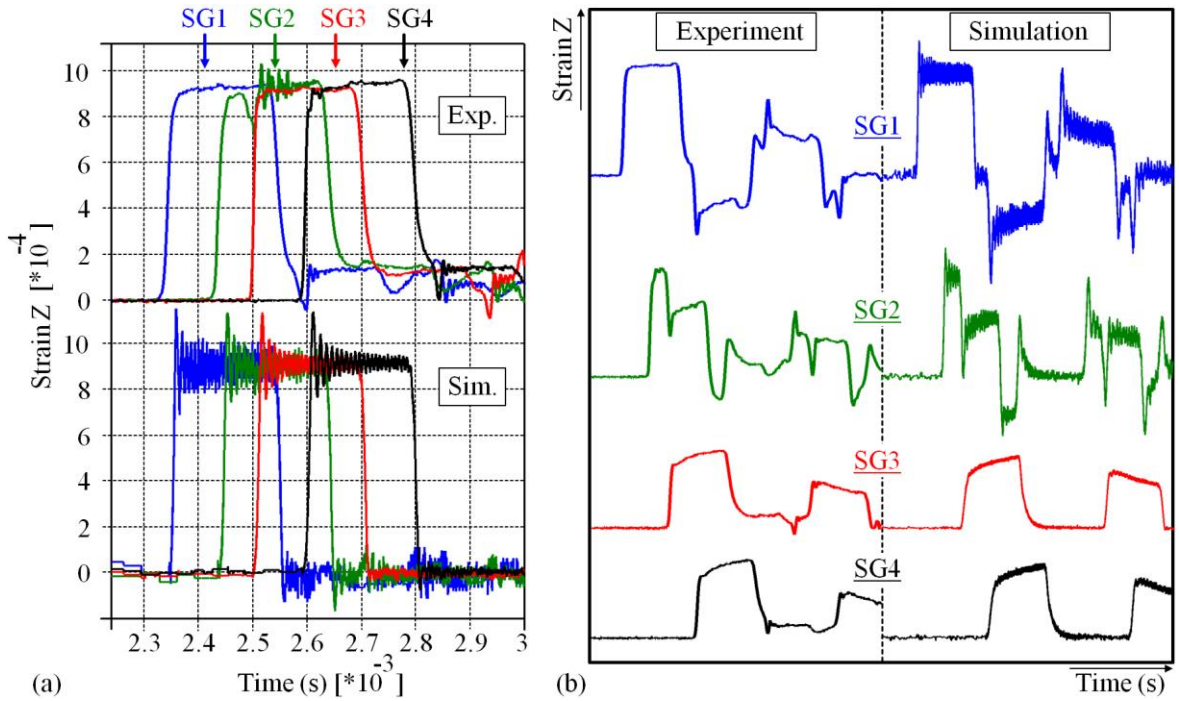

Figure 4. (a) Propagation of elastic wave pulses during a test shot. The experimental results (top, measured while using a pulse shaper) and of the simulation (bottom) present only the input and output signals in the SHPB setup. (b) The experimental (left) and simulated (right) input, reflected and transmitted signals of a SHPB test with a C75 compression specimen shown at four different SGs, are in excellent agreement.

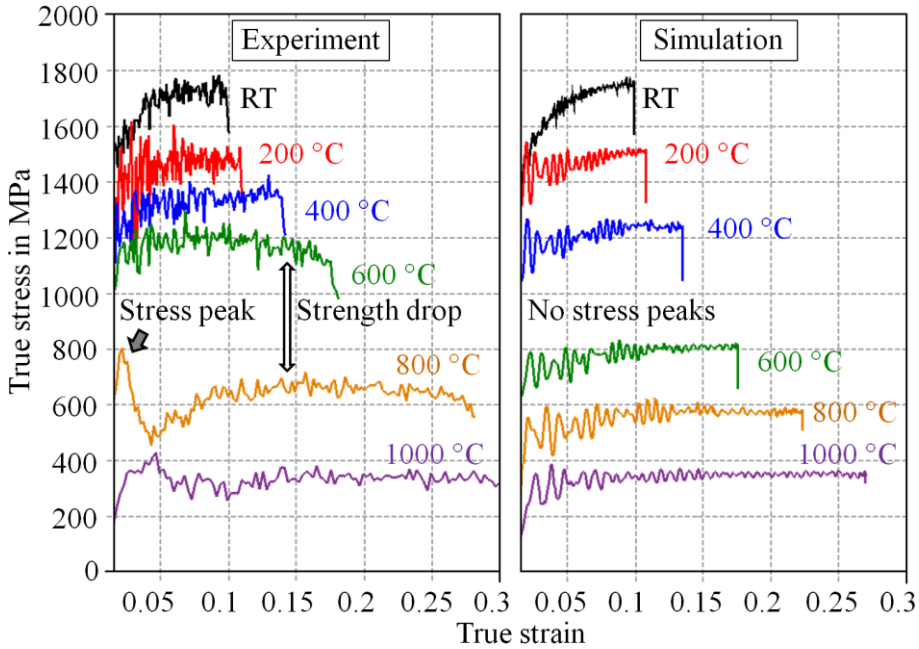

Figure 5. Experimental (left) and numerical (right) true stress-strain curves of the C75 compression specimen under dynamic compressive loading at high strain rates in a SHPB setup at RT and at higher temperatures of 200 °C, 400 °C, 600 °C, 800 °C and 1000 °C.

While the experimental and numerical results are generally in good agreement, a significant strength drop between 600 and 800 °C is observed in the experiments. This strength drop, however, is not included in the simulations as our rather the simple elastic-plastic material model based on the quasi-static results was used for the dynamic simulations. While our material model does predict a gradual decrease of material strength with increasing temperature, the abrupt drop specifically in the temperature range between 600 and 800 °C warrants further microstructural investigation. In the C75 steel, temperatures up to 600 °C are not expected to lead to significant microstructural changes compared to the initial material state at RT. The pronounced strength drop between 600 and 800 °C, however, indicates the onset of the diffusion-controlled phase transformation to austenite at higher temperatures. The micrographs (taken from SHBP specimens after mechanical testing at the corresponding elevated temperatures) shown in figure 6 provide direct microstructural evidence for this phase transition. While the material at 600 °C exhibits the typical features of a tempered martensitic/ bainitic steel, the short heating process (5 s) to 800 °C prior to the dynamic mechanical testing leads to an intermediate bainitic/ austenitic microstructure. In contrast, after fast heating to 1000 °C, the microstructure is austenitic (figure 6c, brighter areas), with additional features of hard pearlite (figure 6c, darker areas).

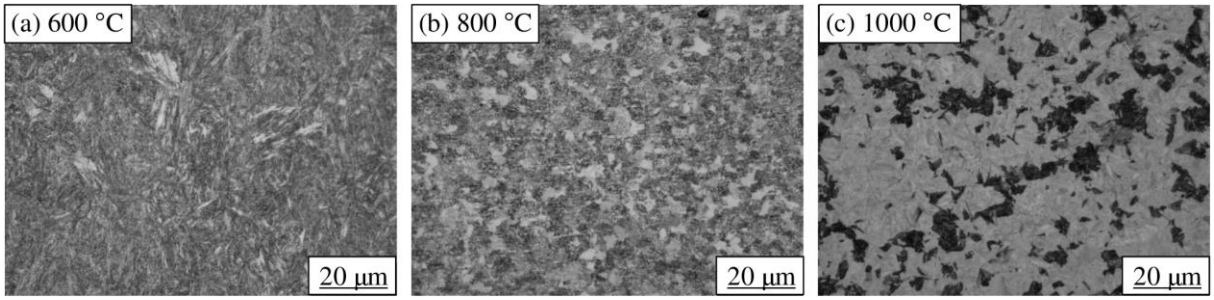

Figure 6. Optical micrographs of the microstructures in specimens deformed at different temperatures in the SHPB setup. (a) While the microstructure remains stable up to 600 °C and exhibits mainly martensitic and bainitic features, (b) heating to 800 °C leads to a bainitic/ austenitic microstructure, whereas (c) heating to 1000 °C results in an austenitic (brighter areas) / hard pearlite (darker areas) microstructure.

4. Summary and Conclusions

In this paper, we have characterized temperature effects on the compressive deformation behavior of the carbon steel C75 under quasi-static uniaxial loading and, most importantly, under dynamic loading conditions. The experimental findings were compared to finite element simulations using a simple elastic-plastic material model. Our main results can be summarized as follows:

1. When a “test shot” without a specimen is performed, it is possible to verify the simulation of wave propagation in the SHPB setup, and experimental and numerical results are in excellent agreement. The simulated input, reflected and output signals including deformation of a C75 specimen in the SHPB also agree well with those of actual experiments.
2. Different parameters, i.e., the effect of geometry and detailed setup of the SHPB (e.g. the use of ceramic plates) can be also considered during finite element simulations. Thus, the true dynamic mechanical response of the C75 specimen at room temperature and at higher temperatures up to 1000 °C can be studied both experimentally and numerically.
3. A strength drop in the true stress-strain curves (between 600 and 800 °C) and at high strain rates is observed experimentally. This effect can be related to the diffusion-controlled phase transformation to austenite at higher temperatures, which is not included in our finite element simulations.

References

[1] Meyer L W, Weise A and Hahn F 1997 Comparison of constitutive flow curve relations in cold and hot forming *J. Physique IV* **7(C3)** 13–20
[2] Lee Y, Kim B M, Park S W and Min O 2002 A study for the constitutive equation of carbon steel subjected to large strains, high temperatures and high strain rates *J. Mater. Process. Technol*. **130–131** 181–8
[3] Sellars C M 1990 Modelling microstructural development during hot rolling *Mater. Sci. Technol*. **6** 1072–81
[4] Wang M, Li X, Du F and Zheng Y 2005 A coupled thermal–mechanical and microstructural simulation of the cross wedge rolling process and experimental verification *Mater. Sci. Eng.* A **391** 305–12
[5] Pinheiro I P, Barbosa R and Cetlin P R 2007 The relevance of dynamic recrystallization in the hot deformation of IF steel at high strain rates *Mater. Sci. Eng.* A **457** 90–3
[6] Dehghan-Manshadi A, Barnett M R and Hodgson P D 2008 Hot deformation and recrystallization of austenitic stainless steel. Part I: Dynamic recrystallization. *Metall. Mater. Trans.* A **39** 1359–70
[7] Meyer L W, Kuprin C and Halle T 2009 High rate material behaviour at hot forming conditions *J. Mech. Time-Depend. Mater.* **13** 49–62
[8] Halle T 2009 Ermittlung und Modellierung von Werkstoffkenndaten metallischer Werkstoffe bei hohen Dehnungsgeschwindigkeiten *Habilitation Thesis* TU Chemnitz